High resolution UV spectroscopy of phenol and the hydrogen bonded phenol-water cluster

Giel Berden and W. Leo Meerts
Department of Molecular and Laser Physics, University of Nijmegen, Toernooiveld, 6525 ED Nijmegen, The Netherlands

Michael Schmitt and Karl Kleinermanns
Inst. für Physikalische Chemie und Elektrochemie I, Heinrich-Heine Universität, Universitätsstr. 26.43.02, 40225 Düsseldorf, Germany

(Received 17 July 1995; accepted 10 October 1995)

The $S_1 \leftarrow S_0$ 0_0^0 transitions of phenol and the hydrogen bonded phenol$(H_2O)_1$ cluster have been studied by high resolution fluorescence excitation spectroscopy. All lines in the monomer spectrum are split by 56 ± 4 MHz due to the internal rotation of the $-$OH group about the a axis. The barrier for this internal motion is determined in the ground and excited states; $V_2'' = 1215$ cm^{-1}, and $V_2' = 4710$ cm^{-1}. The rotational constants for the monomer in the ground state are in agreement with those reported in microwave studies. The excited state rotational constants were found to be $A' = 5313.7$ MHz, $B' = 2620.5$ MHz, and $C' = 1756.08$ MHz. The region of the redshifted 0_0^0 transition of phenol$(H_2O)_1$ shows two distinct bands which are 0.85 cm^{-1} apart. Their splitting arises from a torsional motion which interchanges the two equivalent H atoms in the H_2O moiety of the cluster. This assignment was confirmed by spin statistical considerations. Both bands could be fit to rigid rotor Hamiltonians. Due to the interaction between the overall rotation of the entire cluster and the internal rotation, both bands have different rotational constants. They show that $V_2' < V_2''$, and that the internal rotation axis is nearly parallel to the a-axis of the cluster. If it is assumed that the structure of the rotor part does not change upon electronic excitation, the internal motion becomes simply a rotation of the water molecule around its symmetry axis. Assuming this motion, barriers of 180 and 130 cm^{-1} could be estimated for the S_0 and S_1 states, respectively. The analysis of the rotational constants of the cluster yielded an O–O distance of the hydrogen bond of 2.93 Å in the ground state and 2.89 Å in the electronically excited state. In the equilibrium structure of the cluster, the plane containing phenol bisects the plane of the water molecule. © *1996 American Institute of Physics.* [S0021-9606(96)01703-1]

I. INTRODUCTION

High resolution laser spectroscopy in strongly collimated molecular beams is a powerful tool for the spectroscopic investigation of hydrogen bonded systems.[1] An important model system is the phenol$(H_2O)_1$ cluster, which has been studied extensively both experimentally and theoretically. In the preceding publication, the ground state geometry of the phenol$(H_2O)_1$ cluster has been determined by microwave (MW) spectroscopy in a molecular beam.[2] In this section the high resolution UV spectrum of the $S_1 \leftarrow S_0$ transition of phenol$(H_2O)_1$ is presented.

A. Phenol

An interpretation of cluster spectra has to be preceded by a careful examination of the monomer properties. The ground state rotational constants of phenol and the barrier to internal rotation of the hydroxyl group have been determined by microwave spectroscopy.[3–5] The complete substitution structure has been determined by Larsen.[6] A vibrational analysis of phenol was performed by Bist *et al.*[7–9] using IR and UV-VIS spectroscopy, and by Wilson *et al.*[10] using Raman spectroscopy. The former authors applied the Longuet-Higgins concept of molecular symmetry groups[11] to the phenol molecule. Their group theoretical considerations led to a classification of intramolecular vibrations of phenol under the molecular symmetry group (MS) G_4, which is isomorphic with the point group C_{2v}. The vibrational structure of the electronic ground state of phenol has been studied theoretically at the Hartree–Fock 4-31G and 6-31G** levels.[12] Force field calculations, based on the results of multiphoton ionization photoelectron studies of phenol yielded vibrational frequencies for the $^2B_1$ cation.[13] Recently, the vibrational frequencies of the excited states (S_1 and T_1) of phenol have been evaluated at the complete active space multiconfiguration self-consistent-field (CAS-MCSCF) level, using the 6-31G basis.[14] Kim and Jordan[15] have used many-body perturbation and quadratic configuration interaction calculations with several basis sets to estimate the height of the barrier for OH rotation. Their best estimate of the barrier height was 1076 cm^{-1}.

A rotational band contour analysis of the 275 nm system of phenol has been performed by Christoffersen *et al.*[16] yielding a set of rotational constants for the ground and excited electronic states. A fully rotationally resolved spectrum of phenol was reported by Martinez *et al.*[17] From the experimental rotational parameters they obtained a geometry for both electronic states. With a resolution of 154 MHz, they were able to resolve single rovibronic transitions but could

 0021-9606/96/104(3)/972/11/$6.00

not resolve the torsional doubling. In this paper we report the fully resolved rotational spectrum of phenol obtained in a supersonic molecular beam. Although the linewidth of the spectrometer is only 14 MHz, broad (110 MHz) asymmetric rotational lines were observed due to the short lifetime in the S_1 state and an internal motion of the hydroxyl group.

B. Phenol/water

The vibronic structure of the electronic ground state of phenol/water cluster has been studied by dispersed fluorescence spectroscopy (DF),[18] stimulated emission ion-dip spectroscopy (SEID),[19] ionization-loss stimulated Raman spectroscopy (ILSRS),[20] and IR-UV double resonance spectroscopy.[21] SEID is limited to a region several hundred wave numbers above the electronic ground state 0_0, because it requires a fast relaxation from the examined vibrational levels. Intermolecular vibrations could only be observed as combination bands with higher frequency intramolecular vibrations. Especially the C–O stretching vibration in the phenol moiety and O–H stretching vibrations in phenol and the water moiety have been investigated using ILSRS and IR–UV double resonance spectroscopy.

Laser-induced fluorescence excitation spectra of the $S_1 \leftarrow S_0$ transition in the hydrogen bonded phenol$(H_2O)_1$ cluster have been recorded by Abe *et al.*[22,23] They assigned a vibration at 156 cm^{-1} to the stretching vibration and a band at 121 cm^{-1} to a not further specified S_1 intermolecular bending motion. Other spectral features could not be attributed to the $n=1$ cluster, specifically since the method lacks mass selectivity.

Mass selective spectra of phenol/water clusters with different sizes have been reported by Fuke *et al.*,[24] Stanley *et al.*,[25] and Lipert *et al.*,[26] using resonance enhanced multiphoton ionization (REMPI). The spectral shifts of these clusters were found to resemble those of the similar *p*-cresol$(H_2O)_n$ clusters.[27] The large red shift of phenol $(H_2O)_1$ relative to phenol (353 cm^{-1}) can be attributed to a change in inductive effect of the phenolic oxygen atom on the $\pi^* \leftarrow \pi$ transition, while the second water molecule reduces the inductive effect of the first, proton accepting water and causes a relative blue shift.[28,29] The mass selectivity of REMPI even under ''soft'' ionization conditions is limited by fragmentation of higher clusters, which often obscures the interpretation of the spectra. This problem can be avoided by the employment of spectral hole burning. The vibronic spectra of phenol$(H_2O)_2$ (Ref. 30) and phenol$(H_2O)_3$ (Ref. 31) have been measured cluster and state selectively by this method.

The S_1 life times of phenol and several phenol/water clusters have been measured using time resolved pump–probe photoionization spectroscopy. They were found to vary considerably with cluster size.[32–35] A study of the sensitized phosphorescence spectra of phenol$(H_2O)_n$ clusters was performed by Goto *et al.*[36] Significant phosphorescence was found when the $n=3$ and $n=4$ cluster origins were excited. The phenol$(H_2O)_1$ cation radical was investigated by Dopfer *et al.*[37–39] experimentally using zero-kinetic-energy photoelectron spectroscopy (ZEKE), and theoretically via an *ab initio* study by Hobza *et al.*[40] They used the 0_0^0, the stretching and the in-plane wagging vibration as intermediate S_1 levels for obtaining ZEKE spectra and found an increase in vibrational frequencies in the cation compared to the S_1 state.

A very thorough theoretical and experimental study of the phenol$(H_2O)_1$ cluster was performed by Schütz *et al.*[18] They compared the results of mass selective R2PI and dispersed fluorescence spectroscopy to a vibrational analysis of the cluster based on *ab initio* calculations. A band at 155 cm^{-1} in the electronic ground state was found to correspond to 156 cm^{-1} in the electronically excited state and was assigned to the intermolecular stretching vibration. Furthermore, a band at 146 cm^{-1} in the S_0 state (121 cm^{-1} in the S_1 state) was assigned as the totally symmetric in-plane wagging motion. In addition, some low frequency bands were attributed to a hindered internal motion in the cluster, a motion that exchanges the two equivalent H atoms in the water moiety.

The assignment of the vibrations associated with this internal motion is difficult due to their low Franck–Condon activity. This indicates that there is no large conformational change along this coordinate when exciting the cluster. High resolution UV spectroscopy can give information about this internal motion since the torsional tunneling splitting can be measured directly. Additional information about the potential barrier of this motion is obtained from the rotational constants since these are perturbed by an interaction between the overall rotation of the molecule and the internal motion.

II. THEORY

A. Internal rotation with a twofold barrier

In this section the Hamiltonian will be derived which describes all spectral features in the high resolution spectra of phenol and phenol$(H_2O)_1$. Whenever the word 'molecule' is used, the reader should keep in mind that the theory describes a molecular complex as well. We assume that the entire molecule consists of two parts: a rigid rotor attached to a rigid frame. The two rigid parts rotate relative to each other, generating torsional level structure. Other modes of internal motion are ignored. Furthermore, the entire molecule rotates in space generating rotational level structure.

For the description of internal rotation, we use the principal axis method (PAM).[41] In this method, the principal inertial axes of the whole molecule are used as reference coordinate system. The PAM has been developed for systems in which the rigid rotor part is a symmetric top (e.g., CH_3) and the axis of internal rotation coincides with the symmetry axis of this top. Because of the symmetry of the top, the principal axes and the moments of inertia of the entire molecule are not altered by the rotation of the top relative to the frame.

For bare phenol, the rotating $-OH$ group is asymmetric with respect to the axis of internal rotation (*a* axis of the molecule). However, the moment of inertia of the hydroxyl group about the internal rotation axis is very small compared to that of the C_6H_5 group. Therefore, the principal axes and

moments of inertia of the whole molecule are only very slightly altered by the rotation of the hydroxyl group. Thus we can assume that the hydroxyl group is "symmetric," and the PAM can be used. With analogous arguments, we assume that the water molecule in the phenol$(H_2O)_1$ cluster can be considered to behave as a "symmetric" top.

It is further assumed that the coupling between the torsional motion and the overall rotation is small and can be treated by perturbation theory. The total Hamiltonian can then be divided into three parts:[41]

$$H=H_t+H_r+H_{tr}. \tag{1}$$

The terms H_t and H_r are, respectively, the torsional and rotational part, and H_{tr} describes the coupling between the angular momenta of internal and overall rotation.

The torsional potential is assumed to be one dimensional, depending only on the angle α describing the internal motion. This twofold barrier potential $V(\alpha)$ can be expanded in a Fourier series. If the expansion is restricted to the lowest order term, the torsional Hamiltonian is given by

$$H_t=Fp^2+\frac{V_2}{2}\,(1-\cos 2\alpha), \tag{2}$$

where

$$F=\hbar^2/2\gamma I_\alpha \tag{3}$$

and

$$\gamma=1-\sum_g \lambda_g^2 I_\alpha/I_g\,. \tag{4}$$

In these expressions, V_2 is the barrier height of the twofold potential along the torsional coordinate, and p is the total angular momentum of the internal rotor about the axis of rotation ($p=-i\hbar\partial/\partial\alpha$). F depends on the geometry of the system; I_α is the moment of inertia of the rotor about the rotation axis, λ_g are the direction cosines for the orientation of the rotation axis with respect to the principal axes ($g=a,b,c$), and I_g are the principal moments of inertia of the entire molecule. Solving the eigenvalue problem associated with H_t gives the energy eigenvalues $E_{\nu\sigma}$. Each torsional level ν consists of two sublevels ($\sigma=0,1$), whose degeneracy is removed by tunneling through the twofold barrier. The eigenfunctions can be expressed in terms of the free rotor basis functions $e^{im\alpha}$:

$$|\nu,\sigma\rangle=\sum_{k=-\infty}^{\infty} A_k^{(\nu)} e^{i(2k+\sigma)\alpha}. \tag{5}$$

The rigid rotor Hamiltonian H_r is given by

$$H_r=AP_a^2+BP_b^2+CP_c^2, \tag{6}$$

where $A=\hbar^2/2I_a$, etc., and P_g are the components of the total angular momentum along the principal axes. The torsional Hamiltonian has been treated by perturbation theory up to second order. If $W_{\nu\sigma}^{(1)}$ and $W_{\nu\sigma}^{(2)}$ are the first- and second-order perturbation coefficients, H_{tr} can be written as[41]

$$H_{tr}^{\nu\sigma}=FW_{\nu\sigma}^{(1)}(\rho_aP_a+\rho_bP_b+\rho_cP_c)+FW_{\nu\sigma}^{(2)}(\rho_aP_a+\rho_bP_b+\rho_cP_c)^2 \tag{7}$$

with $\rho_g=\lambda_g I_\alpha/I_g$. ν labels the torsional state and σ labels the subtorsional level. The W coefficients depend on the ratio V_2/F and are given by

$$W_{\nu\sigma}^{(1)}=-2\langle\nu,\sigma|p|\nu,\sigma\rangle, \tag{8}$$

$$W_{\nu\sigma}^{(2)}=1+4F\sum_{\nu'}\frac{|\langle\nu,\sigma|p|\nu',\sigma\rangle|^2}{E_{\nu\sigma}-E_{\nu'\sigma}}, \tag{9}$$

in which $E_{\nu\sigma}$ are the energy eigenvalues and $|\nu,\sigma\rangle$ are the eigenfunctions of the pure torsional Hamiltonian (Eq. 2). Since the $W_{\nu\sigma}^{(1)}$ coefficients are zero for nondegenerate states, the terms linear in P_g disappear in Eq. (7). After separation of the terms in Eq. (1), H_r and H_{tr} can be combined to give an effective rotational Hamiltonian:

$$\begin{aligned}H_{\rm eff}^{\nu\sigma}&=H_r+H_{tr}^{\nu\sigma}\\&=AP_a^2+BP_b^2+CP_c^2+FW_{\nu\sigma}^{(2)}(\rho_a^2P_a^2+\rho_b^2P_b^2+\rho_c^2P_c^2)\\&\quad+FW_{\nu\sigma}^{(2)}(2\rho_a\rho_bP_aP_b+2\rho_a\rho_cP_aP_c+2\rho_b\rho_cP_bP_c).\end{aligned} \tag{10}$$

The last term containing the cross terms can be neglected since its effect on the energy level spacings is small. The first and second three terms can then be combined to give

$$H_{\rm eff}^{\nu\sigma}=A_{\nu\sigma}P_a^2+B_{\nu\sigma}P_b^2+C_{\nu\sigma}P_c^2, \tag{11}$$

where

$$A_{\nu\sigma}=A+FW_{\nu\sigma}^{(2)}\rho_a^2, \tag{12}$$

$$B_{\nu\sigma}=B+FW_{\nu\sigma}^{(2)}\rho_b^2, \tag{13}$$

$$C_{\nu\sigma}=C+FW_{\nu\sigma}^{(2)}\rho_c^2. \tag{14}$$

The result for a given (ν,σ) state is an effective rigid rotor Hamiltonian with effective rotational constants depending on the particular state. The total energy of a torsional-rotational level is then given by the sum of $E_{\nu\sigma}$ and the eigenvalues of the effective rigid rotor Hamiltonian:

$$E(\nu,\sigma,J,K_a,K_c)=E_{\nu\sigma}+E_{\rm eff}^{\nu\sigma}(J,K_a,K_c). \tag{15}$$

We will now consider the effects of the torsional motion on the observed optical spectra. First of all, because of the use of a jet expansion, only the two subtorsional levels $\sigma=0$ and $\sigma=1$ in the lowest torsional state $\nu=0$ are populated. If the molecules are excited to the origin of the first electronically excited state, the spectrum will consist of two bands ($\sigma'=0\leftarrow\sigma''=0$ and $\sigma'=1\leftarrow\sigma''=1$, see Sec. II B) separated by $\Delta E=(E'_{01}-E''_{01})-(E'_{00}-E''_{00})$. Both bands have different effective rotational constants given by Eqs. (12)–(14). Information about the barrier height V_2 and the geometry of the internal rotor F in the ground and excited can be derived from the energy difference ΔE and the effective rotational constants.

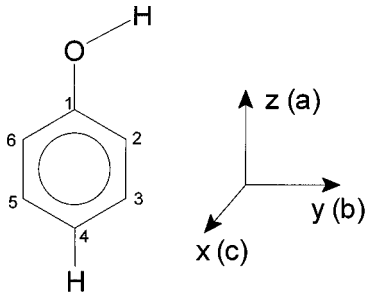

FIG. 1. Definition of structural parameters and axis convention for phenol.

B. Application of the molecular symmetry group G_4 to phenol

The hydroxyl group of phenol undergoes an internal torsional motion relative to the phenyl group. The molecular symmetry (MS) group which takes this motion into account is G_4. This group consists of four elements: the identity operator E, the permutation operator $P=(26)(35)$ which exchanges the identical nuclei (see Fig. 1), the inversion operator E^* of the spatial coordinates of the entire molecule through its center of mass and finally, the permutation inversion operator $P^*=PE^*$. Table I gives the character table of G_4, while Fig. 1 shows our axis conventions.

For phenol the total wave function must have even parity for the exchange of two pairs of equivalent protons at the aromatic ring. The overall wave function must therefore transform as A_1 or A_2:

$$\Gamma_{\text{tot}}=\Gamma_e\otimes\Gamma_v\otimes\Gamma_t\otimes\Gamma_r\otimes\Gamma_{ns}\subset A_1,A_2. \tag{16}$$

In a supersonic molecular beam, the molecules are in the lowest vibrational level of the electronic ground state, thus $\Gamma_e=A_1$ and $\Gamma_v=A_1$. In the following, the characters of the torsional states (Γ_t), the rotational states (Γ_r), and the nuclear spin functions (Γ_{ns}) will be determined.

The symmetry properties of the torsional wave functions [Eq. (5)] depend on the effects of the elements of G_4 on the torsional angle α. This angle can be defined using the Euler angles of the frame (θ_f,ϕ_f,χ_f) and the rotor (θ_r,ϕ_r,χ_r). The frame fixed axis system is chosen parallel to the principal axes of phenol as shown in Fig. 1. The rotor fixed axis system is chosen such that the z axis coincides with that of the frame. Thus $\theta_f=\theta_r=\theta$ and $\phi_f=\phi_r=\phi$. The torsional angle α is defined as $\alpha=\chi_r-\chi_f$.

The effects of the elements of G_4 on the Euler angles can be determined by replacing each element of G_4 by its equivalent rotation.[42] The operation P corresponds to a rotation by π about the a axis (z axis) of the frame, but it does not alter the rotor. E^* corresponds to a rotation by π around the c axis (x), and P^* corresponds to a rotation by π around the b axis (y). The effects of these rotations on the Euler angles are given by Bunker[42] and are summarized in Table II.

TABLE I. Character table for the molecular symmetry group G_4.

	E	P	E^*	P^*	
A_1	1	1	1	1	z
A_2	1	1	−1	−1	
B_1	1	−1	−1	1	x
B_2	1	−1	1	−1	y

TABLE II. Transformation properties of the Euler angles and the internal rotation angle α under the elements of G_4. α is defined as $\alpha=\chi_r-\chi_f$.

E	P	E^*	P^*
θ	θ	$\pi-\theta$	$\pi-\theta$
ϕ	ϕ	$\pi+\phi$	$\pi+\phi$
χ_f	$\pi+\chi_f$	$-\chi_f$	$\pi-\chi_f$
χ_r	χ_r	$-\chi_r$	$-\chi_r$
α	$\alpha-\pi$	$-\alpha$	$-\alpha-\pi$

The application of G_4 to the torsional wave functions will first be described in the free rotor limit ($V_2=0$). The wave functions in this limit are given by $|\psi_m\rangle^{\pm}\propto(e^{im\alpha}\pm e^{-im\alpha})$ and the energy by $E_m\propto m^2$. Using the effects of the elements of G_4 on α (Table II) gives the characters for different m: $\Gamma(m=0)=A_1$, $\Gamma(m=\text{even})=A_1+A_2$ and $\Gamma(m=\text{odd})=B_1+B_2$. All levels with $|m|>0$ are doubly degenerate.

In the high barrier limit ($V_2=\infty$), the torsional wave functions can be written as sums or differences of harmonic oscillator wave functions "centered" at the two equilibrium positions of the hydroxyl rotor (0 and π): $|\psi_\nu\rangle^{\pm}\propto[H_\nu(\alpha)\pm H_\nu(\alpha+\pi)]$. The effects of the elements of G_4 on the wave functions are clear, since $H_\nu(-\alpha)=(-)^\nu H_\nu(\alpha)$. The results are: $\Gamma(\nu=\text{even})=A_1+B_2$ and $\Gamma(\nu=\text{odd})=A_2+B_1$.

Figure 2 shows the correlation diagram between the two limiting cases. The symmetry for states with a barrier $0<V_2<\infty$ can be obtained using the noncrossing rule. Apply-

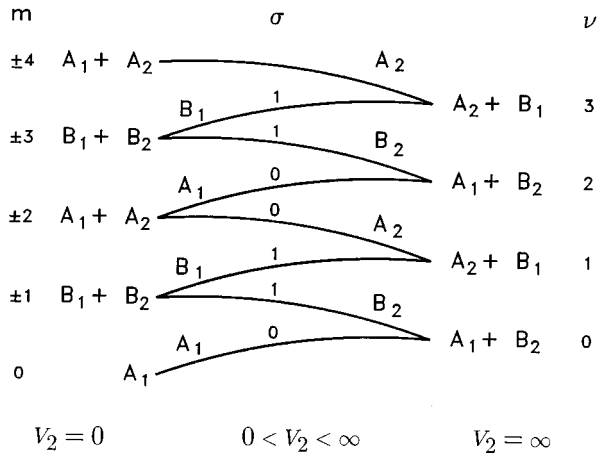

FIG. 2. Correlation between the energy levels of a free rotor ($V_2=0$) and those of a harmonic oscillator ($V_2=\infty$). The quantum numbers labeling the double degenerate energy levels in these extreme barriers are m and ν, respectively. For intermediate barriers this degeneracy is removed. The levels are then labeled with ν and σ. For each level the symmetry is given under the molecular symmetry group G_4.

ing G_4 to the torsional wave function $|\nu,\sigma\rangle$ [Eq. (5)] shows that the $\sigma=0$ states are of A_1 or A_2 symmetry while the $\sigma=1$ states are of B_1 or B_2 symmetry. In the supersonic molecular beam, only the $\nu=0$ levels are populated. Obviously, the lowest state ($\nu=0$, $\sigma=0$) is of A_1 symmetry. The other subtorsional state ($\nu=0$, $\sigma=1$) is of B_2 symmetry.

For an asymmetric top molecule the rotational eigenfunctions are linear combinations of symmetric top functions which depend on the Euler angles. Since the transformation properties of the Euler angles are known (Table II), we can determine the characters of the rotational eigenfunctions. However, an easier way to determine the characters is the use of the isomorphism between G_4 and $V(a,b,c)$. This latter group, the so-called four-group[41] is used to classify asymmetric rotor wave functions in regard to their symmetry with respect to the principal axes of the molecule. The transformation properties of these asymmetric rotor functions under G_4 can be obtained directly from the Four group, since the G_4 elements can be replaced by equivalent rotations around the principal axes. The results are $\Gamma(K_aK_c=ee)=A_1$, $\Gamma(eo)=A_2$, $\Gamma(oo)=B_1$, and $\Gamma(oe)=B_2$.

The torsion of the $-$OH group generates two pairs of equivalent protons on the aromatic ring. The $16(2^4)$ possible spin functions transform under the symmetry operations of G_4 as $10A_1+6B_2$ ($\Gamma_{\rm ns}$). From Eq. (16) it is clear that the statistical weights affect the relative intensities of different torsional-rotational transitions (the hyperfine sublevels are assumed to be degenerate). Transitions starting from ($\sigma=0$, $K_a=$even) or ($\sigma=1$, $K_a=$odd) have a statistical weight of 10, while transitions starting from ($\sigma=0$, $K_a=$odd) or ($\sigma=1$, $K_a=$even) have a statistical weight of 6.

C. Application of the molecular symmetry group G_4 to phenol$(H_2O)_1$

The water moiety in phenol$(H_2O)_1$ undergoes an internal motion which interchanges the two equivalent hydrogen atoms of the water molecule. The molecular symmetry group which takes this motion into account is G_4 (isomorphic with the molecular point group C_{2v}). G_4 consists of four elements: the identity operator E, the permutation operator $P=(12)$ which exchanges the identical nuclei of the water molecule, the inversion operator E^* and $P^*=(12)E^*$. To determine the symmetry of the (sub)torsional levels, we have to consider the symmetry properties of the torsional basis functions under the elements of G_4. The identity E leaves the torsional angle α unaltered, while the permutation P changes α into $\alpha+\pi$. Application of G_4 to the free rotor and harmonic oscillator wave functions results in the same correlation diagram as shown in Fig. 2. Therefore, ($\nu=0$, $\sigma=0$) is of A_1 symmetry, while ($\nu=0$, $\sigma=1$) is of B_2 symmetry.

The total wave function is antisymmetric with respect to the permutation of the two hydrogen atoms, and therefore of B_1 and B_2 symmetry (the inversion E^* leaves the total wave function unaffected). The rotational wave functions are of A_1 symmetry for $K_aK_c=ee$ and oe and of A_2 symmetry for $K_aK_c=oo$ and eo. The four (2^2) spin functions transform as $3A_1+B_2(\Gamma_{ns})$. Since $\Gamma_e=A_1$, $\Gamma_t(\nu=0,\sigma=0)=A_1$ while $\Gamma_t(\nu=0,\sigma=1)=B_2$, it is clear that the statistical weights affect the relative intensities of different torsional transitions. Transitions arising from $\sigma=0$ have a statistical weight of 1, while transitions arising from $\sigma=1$ have a statistical weight of 3.

III. EXPERIMENT

High resolution LIF spectra of phenol and phenol $(H_2O)_1$ have been recorded by using a narrow bandwidth UV laser in combination with the molecular beam apparatus described in Sec. I. In the case of bare phenol, a molecular beam was formed by passing 0.5 bar argon over a heated sample of phenol (70 °C) and expanding this mixture through a nozzle with a diameter of 75 μm. The nozzle was kept at a slightly higher temperature to prevent condensation of phenol in the orifice. The molecular beam was skimmed twice in a differential pumping system and was crossed perpendicularly with a UV laser beam at about 30 cm from the nozzle.

A molecular beam containing phenol/water clusters was formed by passing 0.5 bar argon over a water sample kept at -10 °C and subsequently by passing this mixture over phenol which was kept at 50 °C. This mixture of phenol, water and argon resulted in the strongest LIF spectrum for the phenol(H_2O) cluster.

UV radiation with a bandwidth of 3 MHz was generated by intracavity frequency doubling in a single mode ring dye laser operating on Rh110. By using a 2 mm thick Brewster cut BBO crystal, 0.2 mW of tunable radiation was obtained. For relative frequency calibration a temperature stabilized Fabry–Perot interferometer with a free spectral range of 75 MHz was used. For absolute frequency calibration, the iodine absorption spectrum[43] was recorded simultaneously. The total undispersed fluorescence was collected by two spherical mirrors and imaged on a photomultiplier which was connected to a photon counting system interfaced to a computer. The instrumental linewidth of our spectrometer is 14 MHz, and is mainly determined by residual Doppler broadening.

IV. PHENOL

A. Results

The high resolution excitation spectrum of the electronic origin of the $S_1\leftarrow S_0$ transition of phenol is shown in Fig. 3. The absolute frequency of the band origin (0 on the scale of the figure) is 36348.71 ± 0.01 cm^{-1}. The spectrum, which can immediately be identified as a b-type band, consists of about 300 lines with a linewidth [full width at half-maximum (FWHM)] of roughly 110 MHz. The line shape is asymmetric and the linewidth is larger than expected from lifetime measurements (the reported lifetime of phenol is 2 ns,[33] which would give a Lorentzian contribution to the linewidth of about 80 MHz. These observations indicate that there is unresolved splitting of the lines.

In the b-type microwave spectrum of phenol, all lines were found to be doublets[3] due to the internal rotation of the hydroxyl group. The observed splittings are independent of

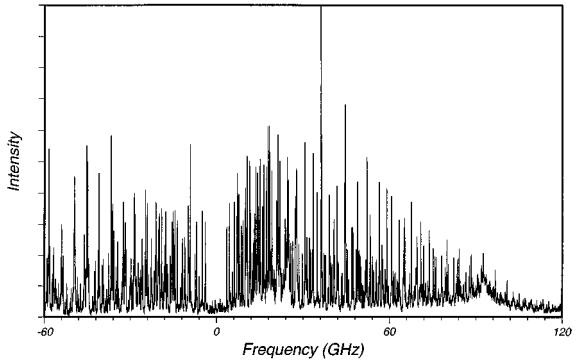

FIG. 3. High resolution LIF spectrum of the origin of the $S_1 \leftarrow S_0$ transition of phenol. The absolute frequency of the origin (0 on the scale of the figure) is a to 36 348.71±0.01 cm^{-1}

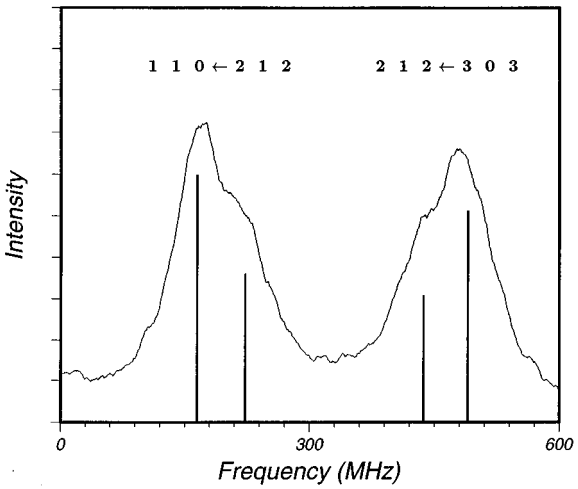

FIG. 4. Enlarge part of the high resolution LIF spectrum (Fig. 3), showing two rotational transitions with different parity for K_a''. The transitions are labeled $(J',K_a',K_c') \leftarrow (J'',K_a'',K_c'')$. The stick spectrum shows that each rotational line is split in two components with an intensity ratio of 10/6. The low frequency components originate from $\sigma=1$, while the high frequency components originate from $\sigma=0$. The subtorsional splitting is 56 MHz.

the rotational transitions. The MW spectrum was fit to a rigid rotor Hamiltonian by using the center frequencies of the doublets. The obtained rotational constants were used as starting values for the rotational assignment of our UV spectrum.

A *b*-type spectrum was simulated using a rigid rotor Hamiltonian with the ground state constants from Ref. 5 and the excited state constants from Martinez *et al.*[17] The latter authors measured the spectrum in a jet with a resolution of 154 MHz. By comparing the simulation with the experimental spectrum, a unique assignment could be made. The center frequencies of the asymmetric lines were used as input for our fitting routine. All lines could be fit within their experimental error. The obtained ground state constants are within their errors equal to the microwave constants.[5] Because the microwave constants are 2 orders of magnitude more accurate than our constants, the UV data were fit again with the ground state constants constrained to the microwave values. The results are shown in Table III; listed are the rotational constants and the inertial defects in the ground and excited states. It should be noted that the values reported by Martinez *et al.*[17] differ considerably from both the MW and our UV results; e.g., their A'' value is 76 MHz larger than our value.

As mentioned earlier, the line shape of the UV lines is asymmetric. Careful examination of the spectrum shows that this asymmetry depends on the parity of K_a, as shown in Fig. 4. Due to internal rotation of the hydroxyl group, the appearance of doublets in the UV spectrum, just as in the microwave spectrum, is expected. Spin statistical considerations predict a 10/6 intensity ratio. For the lowest subtorsional level ($\sigma=0$) in the electronic ground state, even K_a levels have statistical weights of 10 and odd K_a levels have statistical weights of 6, while the opposite holds for $\sigma=1$. Thus, for K_a even the high-frequency component ($\sigma=0$) of the doublet is stronger than the low-frequency component by a factor of 10/6, while for odd K_a the situation is reversed.

The line shapes have been fit using two lines with an intensity ratio of 10:6 and equal linewidths. A Voigt line profile was taken with a fixed Gaussian contribution of 14 MHz (FWHM), which is the instrumental linewidth. Within the experimental error, all line shapes could be fit to this model. The result is a doublet splitting of 56±4 MHz, and a Lorentzian linewidth of 67±8 MHz, both independent of the rotational transition. The Lorentzian linewidth results in a lifetime of 2.4±0.3 ns, which is in agreement with the reported lifetime of 2±1 ns.[33]

The overall shape of the UV spectrum can be simulated using *b*-type selection rules, the rotational constants of Table II, a rotational temperature of 5 K, and the aforementioned doublet structure. There is no experimental indication of hybrid band structure.

TABLE III. Molecular constants of phenol. The rotational constants A, B, and C (in MHz), and the inertial defect $\Delta I = I_c - I_b - I_c$ (in amu Å^2) in the electronic ground state and the first excited state. Values for the ground state have been obtained by fitting the microwave data from Ref. 5. The centrifugal distortion constants are in kHz: $\Delta_J=0.14(3)$, $\Delta_{JK}=0.1(2)$, $\Delta_K=0.9(1)$, $\delta_J=0.03(1)$, and $\delta_K=0.4(3)$ kHz. Every rotational line is split by 56 MHz due to an internal motion in phenol.

A''	5650.515(6)	A'	5313.6(2)
B''	2619.236(3)	B'	2620.5(1)
C''	1789.855(3)	C'	1756.10(4)
$\Delta I''$	−0.0309(5)	$\Delta I'$	−0.18(1)
Doublet splitting	56±4 MHz		
Band origin	36 348.71±0.01 cm^{-1}		

B. Internal rotation and structure

The torsional level structure in the electronic ground state of phenol is well known.[3,4,8] The *b*-type microwave spectrum shows a doublet splitting of 112 MHz.[3] Since the selection rules in this case are $\Delta\sigma=\pm1$, this leads to a splitting of 56 MHz between the subtorsional levels (see Fig. 5). The torsional structure in the ground state has been determined by infrared and ultraviolet absorption spectroscopy up

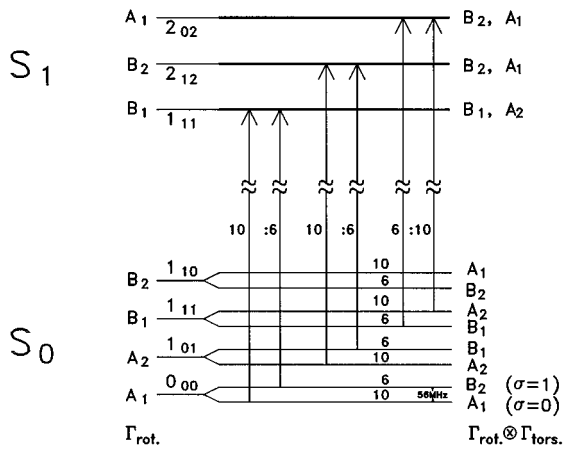

FIG. 5. Energy level scheme for the phenol monomer.

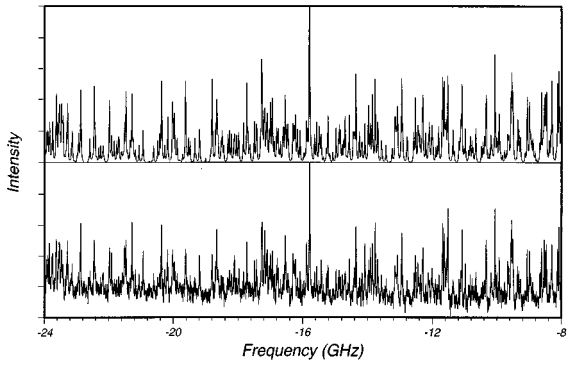

FIG. 6. Part of the high resolution LIF spectrum of the $S_1 \leftarrow S_0$ transition of phenol $(H_2O)_1$ (lower panel). The spectrum consists of two bands originating from different subtorsional levels in the S_0 state. The absolute frequency of the origin of the $\sigma=1$ state (0 on the scale of Figs. 6 and 7) is at $35\,996.47 \pm 0.01$ cm^{-1}. The origin of the $\sigma=0$ state is at -25.455 GHz. The upper panel shows the simulated spectrum.

to $\nu=3$.[8,9] The pure torsional transition $\nu=1\leftarrow 0$ is reported at 309.6 cm^{-1}.[8] This value and the microwave splitting have been used to fit both V_2 and F to Eq. (2). The results are $V_2=1215\pm10$ cm^{-1} and $F=690\pm1$ GHz.

Since the doublet splitting in the UV spectrum is 56 ± 4 MHz, and thus nearly equal to the subtorsional splitting in the electronic ground state, it should be concluded that the torsional splitting in the excited S_1 state is smaller than 4 MHz. This value gives a lower limit of 1700 cm^{-1} for the barrier assuming the same F value as in the S_0 state. From their assignment of the 2750 Å band system of phenol, Bist *et al.*[9] determined the value of the torsional vibration $(\nu'=1\leftarrow 0)$ to be 634.7 cm^{-1}. With the same F value as used above, this gives a barrier of 4710 ± 30 cm^{-1} (with a predicted subtorsional splitting smaller than 1 kHz). The barrier to internal rotation in the excited state is more than three times higher than in the ground state. This may be due to an increase in the double bond character of the C–O bond.

The structure of phenol in the S_0 state has been determined by Larsen.[6] All C–C distances are nearly equal (1.393 Å), as are the C–H distances (1.083 Å). The CCC angles at positions 1, 3, and 5 are 120.7°, and at 2, 6, and 4 are 119.3°. In the hydroxyl group, the oxygen and the hydrogen atoms are on either side of the line through C_1 and C_4. The positions of the oxygen and hydrogen atoms in the principal axes system of phenol (Fig. 1) are $y_O=-0.055(3)$ Å, $z_O=2.283(2)$ Å, and $y_H=0.838(5)$ Å, $z_H=2.629(4)$ Å.

The geometry of the rotor is determined by the value of F which depends on the moment of inertia of the rotor around the internal rotation axis [Eq. (3)]. If it is assumed that the internal rotation axis coincides with the a axis of phenol, the F value can be calculated from the positions of the O and H atoms. The result is $F=674\pm9$ GHz. If the internal rotation axis coincides with the C–O bond, $F=610\pm8$ GHz is calculated using the COH angle and the OH bondlength given by Larsen[6] [108.8(4)° and 0.957(6) Å]. If we compare the calculated values with the value $F=690$ GHz obtained from the fitting of the torsional levels, we conclude that the internal rotation axis is nearly parallel to the a axis.

To elucidate qualitatively the structural changes in phenol upon electronic excitation, we have performed calculations to determine the structure in the S_1 state. The C–O bond decreases upon excitation, since phenol is a stronger acid in the S_1 state than in the S_0 state. Starting with the S_0 geometry from Larsen,[6] we could match the rotational constants in the excited state by increasing the C_1C_2, C_3C_4, C_4C_5, C_6C_1 distances by 0.052 Å, the C_2C_3, C_5C_6 by 0.049 Å, and decreasing the C–O bondlength by 0.118 Å, while leaving the other parameters unaffected. This geometry change is not unique, but is merely an example of a change which is consistent with the measured rotational constants and the increase in acidity. This change in structure in the C_6H_5 group and the decrease in C–O bondlength points to a partially quinoidal structure in the first electronically excited state of phenol. Similar changes in rotational constants have been observed for hydroquinone,[44] which have been interpreted as an increase in quinoidal character as well.

V. PHENOL/WATER

A. Results

The origin band of the phenol $(H_2O)_1$ cluster is red shifted from the monomer origin by 353 cm^{-1}. Part of the high resolution spectrum of the 0_0^0 transition of phenol $(H_2O)_1$ is shown in the lower panel of Fig. 6. The total spectrum consists of about 3000 fully resolved lines with a linewidth of 21 ± 2 MHz. This leads to a lifetime of 15 ± 4 ns, which is in good agreement with the value of 15 ± 1 ns given by Colson *et al.*[33] The spectrum consists of two *ab*-type hybrid bands with different intensities separated by approximately 0.85 cm^{-1}. Both bands could be fit using rigid rotor Hamiltonians, giving two sets of (effective) rotational constants. The ground state rotational constants of each set are, within experimental error, equal to the values obtained from the microwave work.[2] In order to achieve a better accuracy for the excited state rotational constants, our UV data were refit, keeping the ground state constants fixed to the microwave values. The results are shown in Table IV.

TABLE IV. Molecular constants of phenol/water. The effective rotational constants A, B, and C (in MHz), and the inertial defect $\Delta I = I_c - I_b - I_a$ (in amu Å^2) in the electronic ground state and the first excited state. Values for the ground state are taken from Ref. 2.

	$\sigma=1$	$\sigma=0$
A''	4281.76(1)	4291.49(4)
B''	1092.3254(1)	1092.1445(2)
C''	873.9082(1)	873.7271(2)
$\Delta I''$	−2.3968(6)	−2.086(1)
A'	4167.4(2)	4188.8(6)
B'	1100.63(2)	1100.6(2)
C'	874.85(2)	874.62(6)
$\Delta I'$	−2.77(2)	−1.99(9)
Band origin $\sigma=1$	35 996.47±0.01 cm^{-1}	
(Origin $\sigma=1$)−(Origin $\sigma=0$)	25 455±10 MHz	

A simulation of a part of the UV spectrum, using the molecular constants of Table IV, the aforementioned linewidth, and a rotational temperature of 4 K, is shown in the upper panel of Fig. 6. Both bands are hybrid bands with roughly 83% b-type and 17% a-type character. The higher frequency band is 3 times more intense. Figure 7 shows a deconvolution of the total spectrum to elucidate its structure. Only the b-type transitions are shown. For each band the $\Delta J=0$ and $\Delta J=\pm 1$ transitions are shown separately. It is readily seen that the rotational structure of both bands is very similar.

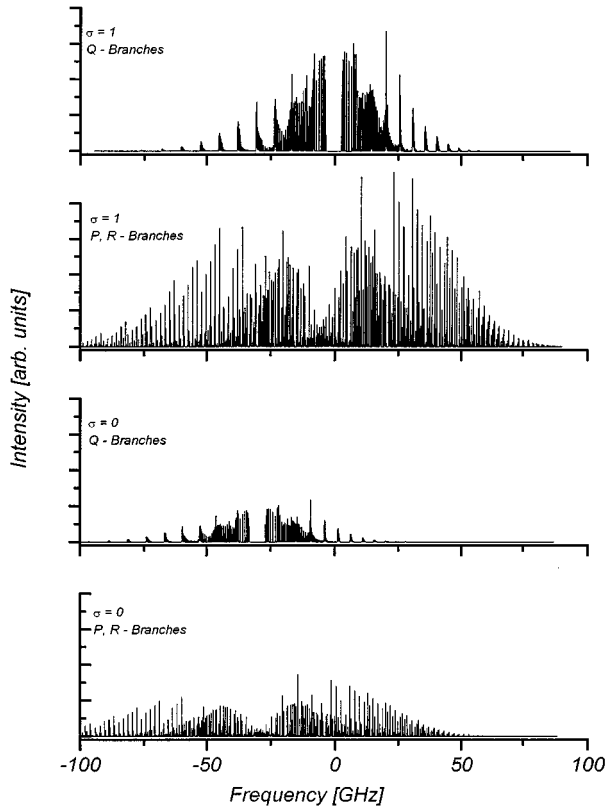

FIG. 7. Deconvolution of the total spectrum to elucidate its structure. Only b-type transitions are shown. For each band the $\Delta J=0(Q)$ and $\Delta J=\pm 1(P,R)$ transitions are shown separately.

B. Internal rotation and structure

The two bands in the UV spectrum of phenol$(H_2O)_1$ arise as a result of the internal torsional motion of the water moiety. Attaching the H_2O quenches the OH torsional motion. A careful comparison of the intensities of both bands shows an intensity ratio of 1:3 of the lower frequency band to the higher frequency band. The results of the spin statistical weights (Sec. II C) leads us to the assignment that the lower frequency band arises from the $\sigma=0$ state, while the higher frequency band arises from the $\sigma=1$ state.

The differences between the effective rotational constants of the $\sigma=0$ and $\sigma=1$ bands are defined as $\Delta A'' = A''_{01} - A''_{00}$ etc., where the double prime denotes the electronic ground state, and the single prime denotes the excited state. The values for the differences can be obtained from Table IV: $\Delta A''=-9.73$ MHz and $\Delta A'=-21.4$ MHz; all other differences are smaller than 0.3 MHz and positive. According to Eqs. (12)–(14), all differences (ΔA, ΔB, and ΔC) should have the same sign. This is not the case, as Table IV shows. Apparently, our assumption that the rotor is ''symmetric'' is not completely valid; the moments of inertia of the cluster change slightly when the water moiety rotates. Since the signs of ΔB and ΔC are opposite to that of ΔA, and their values are small, it is concluded that the internal rotation axis is (nearly) parallel to the a axis of phenol $(H_2O)_1$ in both electronic states (cf. Fig. 10).

Perturbations of the rotational constants (i.e., the difference between effective and ''real'' rotational constants) increase if the reduced barrier height (V_2/F) decreases. Since $|\Delta A'|>|\Delta A''|$, it is concluded that the reduced barrier height in the excited state is smaller than in the ground state. As a consequence, the subtorsional splitting in the S_1 state is larger than in the S_0 state. The resulting energy level scheme is shown in Fig. 8. Notice that the rational level spacing is smaller than the subtorsional splittings.

The splitting between the two bands observed in the UV spectrum is equal to the *difference* in the subtorsional splittings of the ground and excited states (see Sec. II A). Unfortunately, only a-type transitions have been observed in the MW experiment.[2] These transitions with selection rule $\Delta\sigma=0$ contain no information about the subtorsional splitting.

From the experimental results, we want to determine the values of V_2 and F in the S_0 and S_1 states. Unfortunately, our experiments yield only three pieces of information: $\Delta A''$, $\Delta A'$, and the splitting between the two UV bands. Therefore one parameter has to be fixed. Schütz *et al.*[18] explored the tunneling path of the internal motion by examination of the potential energy surface. Their conclusion was that the internal motion is a rotation of the water molecule about the hydrogen bond (correlating with a rotation about the b axis of H_2O) perturbed by a wagging of the water molecule (correlating with a rotation about the a axis of H_2O). Therefore, we have determined V''_2, V'_2, and F' as a function of F'',

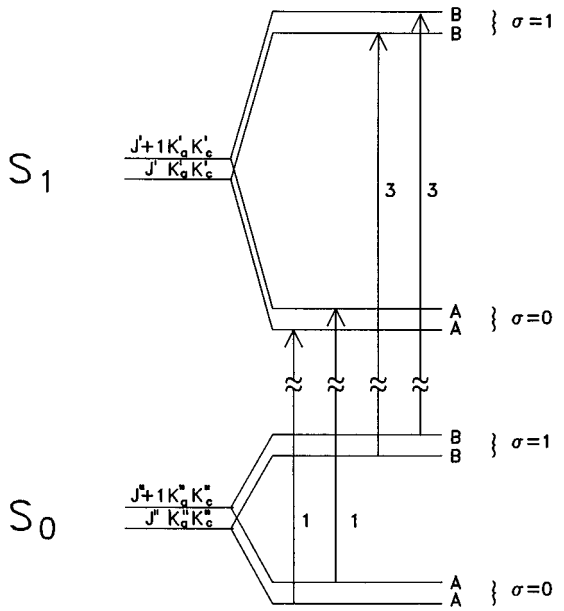

FIG. 8. Energy level scheme for the phenol$(H_2O)_1$ cluster.

which was varied between the B and A rotational constants of water. The results are shown in Fig. 9. The barrier in the excited state is lower than in the ground state ($V_2' < V_2''$) for every value of F''.

If phenol$(H_2O)_1$ is excited to the S_1 state, the transition mainly takes place in the phenol chromophore, since the vibrational structures in the low resolution excitation spectra of the phenol monomer and the cluster are similar.[18] This would indicate that the structural changes upon electronic excitation mainly take place in the phenol part. Therefore, it is expected that there are no (large) structural changes in the rotor part (the water moiety). Therefore, we might expect that $F' \approx F''$. In that case, the F value is 444 GHz (Fig. 9). From Eq. (3) it is seen that $F \approx F_\alpha + A$, in which $F_\alpha = \hbar^2/2I_\alpha$ and A is the rotational constant of phenol$(H_2O)_1$. Since $A=4$ GHz, this gives $F_\alpha = 440$ GHz. This latter value is close to the value of

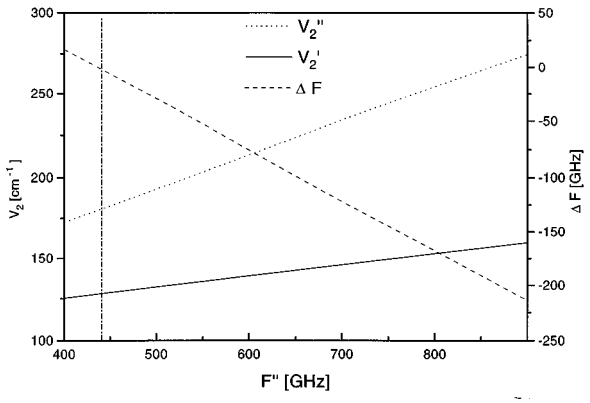

FIG. 9. Internal rotation of the water moiety in phenol$(H_2O)_1$. The barrier heights in the S_0 and S_1 state (V_2'' and V_2', resp.) and the change in geometrical structure of the rotor part ($\Delta F = F' - F''$) as function of the geometrical structure in the S_0 state (F''). The vertical line indicates $\Delta F = 0$.

the rotational B constant of water; 435 GHz.[47] In other words, the logical assumption that the geometry of the rotor does not change upon electronic excitation leads to a very simple picture for the internal motion. The water molecule rotates around its symmetry axis, which is parallel to the a axis of the entire cluster. Using this picture, the barriers for internal rotation are calculated to be (Fig. 9) $V_2'' = 180\ \mathrm{cm}^{-1}$ and $V_2' = 130\ \mathrm{cm}^{-1}$.

To obtain more insight in the direction of the internal rotation axis, we have fit the barrier heights and the direction of the internal rotation axis. Two assumption are now made; the internal rotation axis is in the ab plane and $F'' = F' = 435$ GHz (B rotational constant of water). The result is an angle of 9° with the a axis. The barriers are $V_2'' = 177\ \mathrm{cm}^{-1}$ and $V_2' = 127\ \mathrm{cm}^{-1}$. Since the internal rotation axis has now a component along the b axis, the rotational B constant of the cluster should be perturbed. The difference ΔB is calculated to be -0.04 MHz. We have also fit the data as a function of the angle between the internal rotation axis and the a axis. Now, $F'' = F'$ was a fit parameter. Increasing the angle results in a rapid decrease of F and a rapid increase of the absolute value of ΔB (but ΔB is always negative). From these calculations we estimate that the internal rotation axis makes an angle of less than 20° with the a axis. In the following, we will assume that the internal rotation axis is parallel to the a axis.

In what follows, we want to determine the geometrical structure of phenol$(H_2O)_1$. From Eq. (12) it is seen that the ''real'' rotational constant A can be obtained by subtracting the perturbation term from the effective rotational constant. For a barrier of 180 cm^{-1}, these perturbation terms are 4.7 MHz for $\sigma=0$ and -5.0 MHz for $\sigma=1$, the result is $A''=4286.5$ MHz. It should be noted that the values of the perturbation terms are rather insensitive to the choice of F'',[45] so that this choice does not affect the conclusions about the geometrical structure. The S_1 state with $V_2' = 130\ \mathrm{cm}^{-1}$ gives $A'=4177.4$ MHz.

From the unperturbed rotational constants, the inertial defect can be calculated to be $\Delta I'' = -2.27$ amu Å^2. If the oxygen atom of the water moiety is in the phenyl plane, and if that plane is perpendicular to the plane containing the water molecule, the inertial defect can be calculated from the rotational B constant of water to be $\Delta I''_{\mathrm{calc}} = -2.32$ amu Å^2. We therefore conclude that in the equilibrium structure of the cluster the plane containing phenol bisects the plane of the water molecule. From the internal rotation analysis, it has been concluded that the symmetry axis of the water molecule is nearly parallel to the a-axis of phenol$(H_2O)_1$.

Assuming that the structure of phenol in the phenol$(H_2O)_1$ cluster is identical to the structure of bare phenol, it is possible to calculate the hydrogen bond length, defined by the O–O distance, in the S_0 state without knowing the structure of bare phenol. It should be kept in mind that the validity of this assumption is limited; e.g., a slight shortening of the C–O bond upon cluster formation is predicted by calculations.[18] The O–O distance can be determined if the positions of both oxygen atoms are calculated in the same coordinate system. The origin of this system is chosen at the

center of mass of bare phenol with the axes parallel to its principal axes ($x=c, y=b, z=a$).

The position of the oxygen atom in bare phenol (and therefore in our approximation also in the cluster) has been determined by Larsen[6] and was given in Sec. IV B. The position of the oxygen in the water moiety can be obtained *via* a relationship between the rotational constants of the cluster and the monomer. This method has been used previously by Meerts *et al.* to determine the position of the argon atom in the fluorene-argon van der Waals complex.[46] The inertial tensor elements for the cluster are calculated in the aforementioned coordinate system. The element I_{xx} can be written as

$$I_{xx}=I_{cc}^{p}+\sum_{i=1}^{3} m_i^w (y_i^w)^2-\frac{1}{M_c}\left(\sum_{i=1}^{3} m_i^w y_i^w\right)^2 + \sum_{i=1}^{3} m_i^w (z_i^w)^2-\frac{1}{M_c}\left(\sum_{i=1}^{3} m_i^w z_i^w\right)^2, \tag{17}$$

where x_i^w, y_i^w and z_i^w are the coordinates of the water atoms, M_c is the mass of the entire cluster, and I_{gg}^p are the principal moments of inertia of the phenol monomer ($I_{cc}^p=\hbar^2/2C$). The other diagonal elements, I_{yy} and I_{zz}, can be obtained by cyclic permutation of the coordinates. The off-diagonal term I_{xy} is given by

$$I_{xy}=\frac{1}{M_c}\sum_{i=1}^{3} m_i^w x_i^w \sum_{i=1}^{3} m_i^w y_i^w-\sum_{i=1}^{3} m_i^w x_i^w y_i^w . \tag{18}$$

Cyclic permutation gives the other elements. The only unknown parameters in the tensor are the positions of the atoms in the water moiety, since the moments of inertia of the monomer are known. The positions of the hydrogen atoms in the water moiety can be expressed relative to the position of the oxygen atom, since the structure of water is known [$R_{OH}=0.957$ Å, H–O–H=104.52° (Ref. 47)]. From the inertial defect, it is known that the plane containing phenol bisects the plane of the water moiety, which gives the x-coordinates of the water atoms (for oxygen $x=0$). From the internal rotation analysis, it is known that the symmetry axis of the water molecule is parallel to the a axis of the cluster. Therefore, the only parameters left are the y and z coordinates of the oxygen atom. Diagonalization of the inertial tensor yields the known moments of inertia of the cluster. A least-square fit gives $|y|=2.534(10)$ Å and $|z|=3.653(10)$ Å. This results in a hydrogen bond-length of 2.93(2) Å. Other structural parameters are described in Fig. 10 and given in Table V, together with the *ab initio* results from Schütz *et al.*[18]

In principle, the same procedure could be used to determine the hydrogen bond length in the S_1 state. Unfortunately, no high resolution UV spectrum of isotopically substituted phenols have been recorded yet, so we do not know the position of the oxygen atom in the S_1 state. Therefore, we have used the structure of phenol as obtained by fitting the structure to the rotational constants (Sec. IV B). A good indication for the reliability of our structural assumptions is the equality (within errors) of the calculated S_0 oxygen coordinates with those obtained from substitution experiments. The

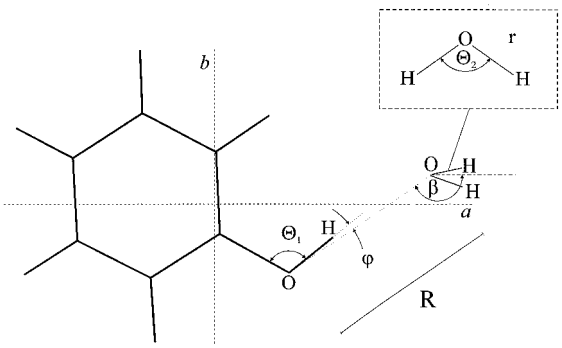

FIG. 10. Definition of structural parameters in phenol$(H_2O)_1$.

results for the phenolic oxygen atom in the S_1 state are $y=-0.063$ Å and $z=2.234$ Å. The position of the water oxygen can be calculated using the method described earlier: $|y|=2.447(20)$ Å and $|z|=3.657(20)$ Å. The hydrogen bond length in the excited state is thus calculated to be 2.89(3) Å, indicating a slight reduction of hydrogen bond length upon electronic excitation. A similar reduction of the bond length upon excitation has been observed in the *trans*-2-hydroxynaphthalene(NH_3) (Ref. 1) and in the *trans*-hydroquinone(NH_3) (Ref. 48). In both cases, the NH_3 rotates about its symmetry axis, and the barriers to this motion increase on electronic excitation.

VI. CONCLUSIONS

In the present high resolution UV study on phenol and the phenol $(H_2O)_1$ cluster in a supersonic molecular beam, the structure and dynamics of internal motions in these molecules could be illuminated. The rovibronic lines of phenol show a splitting due to the strongly hindered internal rotation of the $-$OH group around the a axis of the molecule. The splitting in the UV spectrum is within experimental error equal to the observed splitting in the MW experiments (56 MHz). Therefore, the splitting in the S_1 state is <4 MHz. This indicates that the barrier to internal rotation in the electronically excited state is much higher than in the ground state. This effect is mainly due to an increase in quinoidal character upon electronic excitation which has indeed been found when fitting the rotational constants. Using the values of the torsional transitions ($\nu=1\leftarrow 0$) reported by Bist

TABLE V. Structural parameters of phenol$(H_2O)_1$ as defined in Fig. 10.

	S_0	S_1	Calc.[a]
R	2.93	2.89	2.940
β	144.5	145.6	147.66
ϕ	6.7		3.31
θ_1	108.8[b]		111.80
$\theta_1+\phi$	115.5		115.11
δ[c]	62.1	60.5	

[a]From Ref. 18.
[b]Value for the phenol monomer (Ref. 6).
[c]The angle δ is defined as the angle between the a axis of bare phenol and the hydrogen bondlength.

et al.,[8,9] and assuming that the structure of the rotor part does not change drastically upon excitation, we could fit all data to obtain the barrier height in the ground and first excited states: $V_2'' = 1215\ \mathrm{cm}^{-1}$ and $V_2' = 4710\ \mathrm{cm}^{-1}$. From the Lorentzian contribution to the linewidth of the rotational transitions, the lifetime of phenol could be determined to be 2.4 ± 0.4 ns.

Contrary to phenol, the splitting due to the torsion of the water moiety in phenol$(H_2O)_1$ is much larger than the frequency separation of the rotational lines. Spectroscopically, two bands, which arise from different subtorsional levels in the ground state, are observed with a splitting of $0.85\ \mathrm{cm}^{-1}$. Both bands have different effective rotational constants, due to an interaction between the overall rotation of the entire cluster and the internal rotation. Because the two hydrogen atoms in the water molecule are equivalent, both bands have different statistical weights (1 and 3 for $\sigma=0$ and 1, respectively). Since the electronic transition mainly takes place in the phenol chromophore, we can assume that the structure of the internal rotor part (the water moiety) does not change upon electronic excitation. In this case, the effective rotational constants and the observed splitting can be fit to obtain the barriers for internal rotation and the structure of the rotor in both electronic states. This assumption gives a simple physical picture for the internal motion: the water molecule rotates around its symmetry axis, which is nearly parallel to the *a* axis of the entire cluster. In this case, a barrier of 180 cm^{-1} for the S_0 state and 130 cm^{-1} for the S_1 state could be estimated.

From rotational constants and the results of internal rotor analysis, it has been shown that phenol$(H_2O)_1$ is *trans*-linear, and the plane containing phenol bisects the plane of the water molecule. The hydrogen bond length, defined by the O–O distance, is 2.93(2) Å in the S_0 state, and 2.89(3) Å in the S_1 state. In conclusion, the barrier for internal rotation and the hydrogen bond length decrease upon electronic excitation.

ACKNOWLEDGMENTS

This work was made possible by financial support from the Dutch Foundation for Fundamental Research on Matter (FOM) and from the Deutsche Forschungsgemeinschaft (DFG). We wish to thank Christoph Jacoby for his assistance in working out the spin statistics and Jack van Rooy for experimental assistance. We also want to thank Dr. P. R. Bunker and Dr. J. T. Hougen for helpful discussions on the molecular symmetry group of the phenol-water system.

[1] See, for example, D. F. Plusquellic, X.-Q. Tan, and D. W. Pratt, J. Chem. Phys. **96**, 8026 (1992).
[2] M. Gerhards, M. Schmitt, K. Kleinermanns, and W. Stahl, J. Chem. Phys. preceding paper, **104**, 967 (1996).
[3] T. Kojima, J. Phys. Soc. Jpn. **15**, 284 (1960).
[4] H. Forest and B. P. Dailey, J. Chem. Phys. **45**, 1736 (1966).
[5] E. Mathier, D. Welti, A. Bauder, and Hs. H. Günthard, J. Mol. Spectrosc. **37**, 63 (1971).
[6] N. W. Larsen, J. Mol. Struct. **51**, 175 (1979).
[7] H. D. Bist, J. C. D. Brand, and D. R. Williams, J. Mol. Spectrosc. **21**, 76 (1966).
[8] H. D. Bist, J. C. D. Brand, and D. R. Williams, J. Mol. Spectrosc. **24**, 402 (1967).
[9] H. D. Bist, J. C. D. Brand, and D. R. Williams, J. Mol. Spectrosc. **24**, 413 (1967).
[10] H. W. Wilson, R. W. MacNamee, and J. R. Durig, J. Raman Spectrosc. **11**, 252 (1981).
[11] H. C. Longuet-Higgins, Mol. Phys. **6**, 445 (1963).
[12] M. Schütz, T. Bürgi, and S. Leutwyler, J. Mol. Struct. (Theochem) **276**, 117 (1992).
[13] S. L. Anderson, L. Goodman, K. Krogh-Jespersen, A. Ozkabak, R. Zare, and C. Zheng, J. Chem. Phys. **82**, 5329 (1985).
[14] M. Krauss, J. O. Jensen, and H. F. Hameka, J. Phys. Chem. **98**, 9955 (1994).
[15] K. Kim and K. D. Jordan, Chem. Phys. Lett. **218**, 261 (1994).
[16] J. Christoffersen, J. M. Hollas, and G. H. Kirby, Proc. R. Soc. London, Ser. A **307**, 97 (1968).
[17] S. J. Martinez III, J. C. Alfano, and D. H. Levy, J. Mol. Spectrosc. **152**, 80 (1992).
[18] M. Schütz, T. Bürgi, and S. Leutwyler, J. Chem. Phys. **98**, 3763 (1993).
[19] T. Ebata, M. Furukawa, T. Suzuki, and M. Ito, J. Opt. Soc. Am. B **7**, 1890 (1990).
[20] G. Hartland, B. Henson, V. Venturo, and P. M. Felker, J. Phys. Chem. **96**, 1164 (1992).
[21] S. Tanabe, T. Ebata, M. Fujii, and N. Mikami, Chem. Phys. Lett. **215**, 347 (1993).
[22] H. Abe, N. Mikami, and M. Ito, J. Phys. Chem. **86**, 1768 (1982).
[23] A. Oikawa, H. Abe, N. Mikami, and M. Ito, J. Phys. Chem. **87**, 5083 (1983).
[24] K. Fuke and K. Kaya, Chem. Phys. Lett. **94**, 97 (1983).
[25] R. J. Stanley and A. W. Castleman, J. Chem. Phys. **94**, 7744 (1991).
[26] R. J. Lipert and S. D. Colson, J. Chem. Phys. **89**, 4579 (1988).
[27] K. Wolf, H.-H. Kuge, M. Schmitt, and K. Kleinermanns, Ber. Bunsenges. Phys. Chem. **96**, 1309 (1992).
[28] M. Pohl, M. Schmitt, and K. Kleinermanns, J. Chem. Phys. **94**, 1717 (1991).
[29] M. Gerhards and K. Kleinermanns (unpublished).
[30] R. J. Lipert and S. D. Colson, Chem. Phys. Lett. **161**, 303 (1989).
[31] M. Schmitt, H. Müller, and K. Kleinermanns, Chem. Phys. Lett. **177**, 246 (1994).
[32] A. Sur and P. M. Johnson, J. Chem. Phys. **84**, 1206 (1986).
[33] R. J. Lipert, G. Bermudez, and S. D. Colson, J. Phys. Chem. **92**, 3801 (1988).
[34] R. J. Lipert and S. D. Colson, J. Phys. Chem. **93**, 135 (1989).
[35] R. J. Lipert and S. D. Colson, J. Phys. Chem. **94**, 2358 (1990).
[36] A. Goto, M. Fujii, N. Mikami, and M. Ito, J. Phys. Chem. **90**, 2370 (1986).
[37] G. Reiser, O. Dopfer, R. Lindner, G. Henri, K. Müller-Dethlefs, E. W. Schlag, and S. D. Colson, Chem. Phys. Lett. **181**, 1 (1991).
[38] O. Dopfer, G. Reiser, K. Müller-Dethlefs, E. W. Schlag, and S. D. Colson, J. Chem. Phys. **101**, 974 (1994).
[39] O. Dopfer and K. Müller-Dethlefs, J. Chem. Phys. **101**, 8508 (1994).
[40] P. Hobza, R. Burcl, V. Špirko, O. Dopfer, K. Müller-Dethlefs, and E. W. Schlag, J. Chem. Phys. **101**, 990 (1994).
[41] W. Gordy and R. L. Cook, *Microwave Molecular Spectra*, 3rd ed. (Wiley, New York, 1984).
[42] P. R. Bunker, *Molecular Symmetry and Spectroscopy* (Academic, New York, 1979).
[43] S. Gerstenkorn and P. Luc, *Atlas du Spectroscopie d'Absorption de la Molecule d'Iode* (CNRS, Paris, 1978); S. Gerstenkorn and P. Luc, Rev. Phys. Appl. **14**, 791 (1979).
[44] S. J. Humphrey and D. W. Pratt, J. Chem. Phys. **99**, 5078 (1993).
[45] D. R. Herschbach, J. Chem. Phys. **31**, 91 (1959).
[46] W. L. Meerts, W. A. Majewski, and W. M. van Herpen, Can. J. Phys. **62**, 1293 (1984).
[47] W. S. Benedict, N. Gailar, and E. K. Plyler, J. Chem. Phys. **24**, 1139 (1956).
[48] S. J. Humphrey *et al.* (unpublished).